

COLLECTIVE MONTE CARLO UPDATING IN A HIGH PRECISION STUDY OF THE x - y MODEL

Ulli WOLFF

Institut für Theoretische Physik, Universität Kiel, D-2300 Kiel, F.R. Germany

Received 19 December 1988

We employ a recently developed collective Monte Carlo algorithm to simulate the two-dimensional x - y model at correlation lengths up to 69. No critical slowing down manifests itself in the measured observables. In the high-temperature phase of the model we observe an approach to criticality of the type predicted by Kosterlitz and Thouless and exclude a conventional critical point. The exponent η exceeds $\frac{1}{4}$ for the observed range of correlation lengths. In the spinwave phase we see a variable η and scaling behavior in agreement with the absence of ultraviolet coupling constant renormalization as expected for the abelian model.

1. Introduction

This paper serves the dual purpose of establishing in detail the advantages of a new collective Monte Carlo algorithm [1] and of producing physics results relevant to the recent controversy [2] about the Kosterlitz–Thouless (KT) transition [3, 4]. In a series of by now classical papers KT predicted a rather exceptional kind of phase transition in the $O(2)$ nonlinear σ -model in two dimensions (x - y model). A standard member of its universality class is defined on a periodic square lattice of L^2 sites by the partition function

$$Z = \prod_x \int_{S_{n-1}} d\sigma_x \exp\left(\beta \sum_{x\mu} \sigma_x \cdot \sigma_{x+\mu}\right) \quad (1.1)$$

with $n = 2$. In eq. (1.1) an n -component spin σ_x is integrated at each site over the unit sphere S_{n-1} , and nearest neighbors in the two directions $\mu = 1, 2$ (euclidean space and time) are coupled. Due to an interplay between the spin space S_1 and the 2-dimensional euclidean base space (scaffolded by the lattice) the abelian $n = 2$ model possesses topologically stable vortex configurations. KT predict that there is a critical inverse temperature β_c such that for $\beta < \beta_c$ vortices are thermodynamically important degrees of freedom which occur with a finite density and disorder the system. At β_c this density tends to zero, vortices and antivortices bind more and more strongly as β grows and eventually lose their meaning as relevant dynamical

degrees of freedom. In an approximate renormalization group calculation for small vortex densities KT derive essential singularities at β_c for various physical quantities as a consequence of vortex dynamics. The magnetic susceptibility,

$$\chi = \sum_x \langle \sigma_0 \cdot \sigma_x \rangle, \quad (1.2)$$

for example, is supposed to diverge as

$$\chi \propto \exp[b_\chi (1 - \beta/\beta_c)^{-\nu}] \quad (1.3)$$

for $\beta \nearrow \beta_c$ with $\nu = \frac{1}{2}$ and a nonuniversal b_χ . An analogous behavior is expected for the correlation length $\xi(\beta)$, and the critical exponent $\eta = \frac{1}{4}$ is predicted at β_c such that

$$\chi \propto \xi^{2-\eta} = \xi^{7/4}. \quad (1.4)$$

In the spinwave dominated region above β_c the model is expected to be critical at all β with continuously changing critical exponents. For the O(2)-symmetric two-point function the long-distance behavior is given by

$$\langle \sigma_x \cdot \sigma_y \rangle \propto |x-y|^{-\eta} \quad (1.5)$$

with $\eta = \eta(\beta)$, and $\eta \cong (2\pi\beta)^{-1}$ at large β from pure spinwave dynamics. In other words, the model does not generate a scale in this phase, and the susceptibility diverges with the size of the system as

$$\chi \propto L^{2-\eta(\beta)}, \quad (1.6)$$

if we scale up L at fixed β .

Earlier computer simulations [5] of the $x-y$ model were severely hampered by critical slowing down. They could not study the region $1 \ll \xi$ with a lattice size and statistics sufficient for a first principles test of the KT predictions. A combination of data from relatively small lattices and finite-size scaling assumptions typically led to results consistent with but not necessarily distinctive of the KT picture. Another general problem is, that to verify (1.3) from numerical results, three or, if ν is determined rather than assumed, even four parameters have to be fitted. Since they are strongly correlated, high-quality data and analysis are required. In ref. [2] correlation lengths up to $\xi \cong 6$ have been studied on an 80^2 lattice using the Z(10) clock model that is indistinguishable from the $x-y$ model in this range. The authors conclude that a conventional critical point with χ and ξ diverging as powers of $\beta_c - \beta$ yields a more plausible fit to their data than the KT form. During our own simulation we received a preprint of ref. [6]. An overrelaxation algorithm with reduced slowing down ($\tau \propto \xi^{1.2}$) is used there. Armed with a parallel computer

correlation lengths $\xi \cong 22$ are reached on a 512^2 lattice. The “raw” data, i.e. $\chi(\beta)$ and $\xi(\beta)$, will be seen to be consistent between ref. [6] and the present simulation. We find it both fortunate and comforting that this comparison is available, because two relatively new methods are used in rather extreme regimes. The results of our data analysis differ from ref. [6]. Although we also generally confirm KT, we come nowhere close to the precision of 1 : 500 with which the authors of ref. [6] derive $\nu = \frac{1}{2}$. This is rather surprising as we have more data at our disposal ranging up to $\xi \cong 69$ on 512^2 with comparable errors. The source of this discrepancy is presently not understood (see sect. 3 for more details). As to the algorithmic aspect of this work, we conclude that the problem of slowing down is completely eliminated by the new algorithm [1]. With an average CPU effort of the order of one local Metropolis sweep we produce an independent estimate for long distance correlation functions at any of the correlation lengths studied.

The paper is organized as follows: In sect. 2, the collective algorithm is introduced. It is followed by the presentations and discussions of our data in the vortex phase in sect. 3, and the spinwave phase in sect. 4. An outlook and some conclusions are offered in sect. 5.

2. Collective updating for $O(n)$ σ -models

The new collective algorithm for spin systems has already been briefly described in ref. [1]. Here we derive it in a slightly more formal way. To execute one elementary update step we first choose isotropically a random direction $r \in S_{n-1}$. Only components of σ_x parallel to r will be changed in this step. Next we construct one cluster C – a subset of the lattice sites – that depends globally on $r \cdot \sigma_x$. To this end we may imagine activating each bond $\langle xy \rangle$ on the whole lattice with a probability given locally by

$$p_r(\sigma_x, \sigma_y) = 1 - \exp[\min(0, -2\beta\sigma_x \cdot r\sigma_y \cdot r)]. \tag{2.1}$$

Active bonds are now interpreted in the sense of bond percolation, and the lattice sites are decomposed into a maximal number of mutually unconnected subsets or clusters c_i , $i = 1, \dots, N_c$. This means that there is no chain of active bonds leading from a site in one cluster to a site in any other cluster. The one cluster C is determined by selecting a lattice site x at random and taking $C = c_{i(x)}$, where $c_{i(x)}$ is the cluster containing x . The new spin configuration succeeding σ is $R(r)^C\sigma$ where

$$(R(r)^C\sigma)_x = \begin{cases} R(r)\sigma_x & \text{for } x \in C \\ \sigma_x & \text{for } x \notin C \end{cases} \tag{2.2}$$

and $R(r) \in O(n)$,

$$R(r)\sigma_x = \sigma_x - 2(\sigma_x \cdot r)r, \tag{2.3}$$

is the reflection operation from ref. [1]. The probability of reaching a configuration σ' from σ in this way is

$$W(\sigma \rightarrow \sigma') = \int_{S_{n-1}} dr \sum_{C \in \mathcal{P}} Q_r(\sigma, C) \delta[\sigma', R(r)^C \sigma], \tag{2.4}$$

where \mathcal{P} is the set of all possible clusters on the lattice. In eq. (2.4) the symmetric “functional” δ -function is defined with the normalized invariant measure on the sphere

$$\prod_x \int_{S_{n-1}} d\sigma_x \delta[\sigma, \sigma'] F[\sigma] = F[\sigma'], \tag{2.5}$$

and $Q_r(\sigma, C)$ is the probability of forming cluster C by the above process. It factorizes into

$$Q_r(\sigma, C) = \frac{|C|}{L^2} \prod_{\langle xy \rangle \in \partial C} [1 - p_r(\sigma_x, \sigma_y)] V_r(\sigma, C), \tag{2.6}$$

where $|C|$ is the number of sites in C , and the surface ∂C is the set of nearest neighbor bonds $\langle xy \rangle$ that connect sites $x \in C$ to sites $y \notin C$. In eq. (2.6) the various explicit factors account for the necessity of choosing member C among the clusters c_i and for the fact that for C to be among the c_i its surface bonds must not be activated. The remaining term $V_r(\sigma, C)$ is the probability that the bonds $\langle xy \rangle$ with both $x \in C$ and $y \in C$ are activated such that C gets connected. It is a very complicated function of the activation probabilities inside of C . We shall, however, only need the simple property

$$V_r(\sigma, C) = V_r(R(r)^C \sigma, C) \tag{2.7}$$

which is a trivial consequence of the invariance

$$p_r(R(r)\sigma_x, R(r)\sigma_y) = p_r(\sigma_x, \sigma_y). \tag{2.8}$$

We are now ready to prove detailed balance for transitions between configurations σ and σ' that can actually be mediated by our process,

$$\sigma' = R(r)^C \sigma \Leftrightarrow \sigma = R(r)^C \sigma' \quad \left(\text{since } (R(r)^C)^2 = 1 \right) \tag{2.9}$$

for some r, C . Apart from a set of configurations of measure zero r and C are uniquely fixed by σ, σ' up to the sign of r . Unless $\sigma = \sigma'$ there is a spin $\sigma_x \neq \sigma'_x = R(r)\sigma_x$. If there is another r' such that $\sigma'_x = R(r')\sigma_x$, then r and r' have to be collinear from eq. (2.3). If there is a cluster C' larger than the unique C where σ and σ' differ, then for all $y \in C' \setminus C$ the condition $R(r)\sigma_y = \sigma_y$ implies $r \cdot \sigma_y = 0$ and restricts these configurations to measure zero. Upon using eqs. (2.6), (2.7), and (2.1) we find

$$\begin{aligned} \frac{W(\sigma \rightarrow \sigma')}{W(\sigma' \rightarrow \sigma)} &= \prod_{\langle xy \rangle \in \partial C} \frac{1 - p_r(\sigma_x, \sigma_y)}{1 - p_r(\sigma'_x, \sigma'_y)} \\ &= \exp \left[\beta \sum_{\langle xy \rangle} (\sigma'_x \cdot \sigma'_y - \sigma_x \cdot \sigma_y) \right]. \end{aligned} \tag{2.10}$$

Ergodicity under repeated applications of the elementary updates follows from a simple argument presented in ref. [1]. Also a more efficient implementation is described there which requires only $O(|C|)$ operations for the elementary step flipping C rather than $O(L^2)$ if one first builds all clusters c_i .

We conclude this section by some comments on the connection between the present algorithm and the one by Swendsen and Wang (SW) [7] which in its original form is applicable for $n = 1$. If one flips each c_i independently with $R(r)^{c_i}$ with probability $\frac{1}{2}$ rather than selecting C and flipping it alone, detailed balance holds, too. The special case $n = 1, \beta > 0$ coincides with SW. By eq. (2.1) only sites with like-sign $\sigma_x \cdot r$ aggregate to the same cluster for $\beta > 0$. Then, for $n = 1$, flipping a cluster at random or picking a new global spin orientation on it is identical. If $\beta < 0$ the present algorithm will automatically produce staggered clusters that are flipped. Of course, this case can be trivially mapped back to the ferromagnetic one by $\sigma_x \rightarrow -\sigma_x$ on the odd sublattice, and the algorithm is merely covariant: the transformation on the initial configuration is handed through to its successor. The algorithm as it is formulated here – both flipping single clusters or conditionally all c_i – is also applicable if $\beta \rightarrow \beta_{\langle xy \rangle}$ is bond dependent with arbitrary sign, a case met in the spin glass problem. It is of course open whether clusters form which lead to good relaxation behavior. As discussed in ref. [1] an important feature of the one-cluster selection method with probability given by the size is that more CPU time goes into moving large clusters. We exclusively used this method implemented as described in ref. [1] for our $x-y$ model simulation whose results follows.

3. Numerical results in the vortex phase

In the vortex phase we performed simulations of the $x-y$ model in a range of β chosen such that the condition $1 \ll \xi \ll L$ is fulfilled for the correlation length ξ . The dependence of ξ on β is plotted in fig. 1 for lattices of various sizes, and some

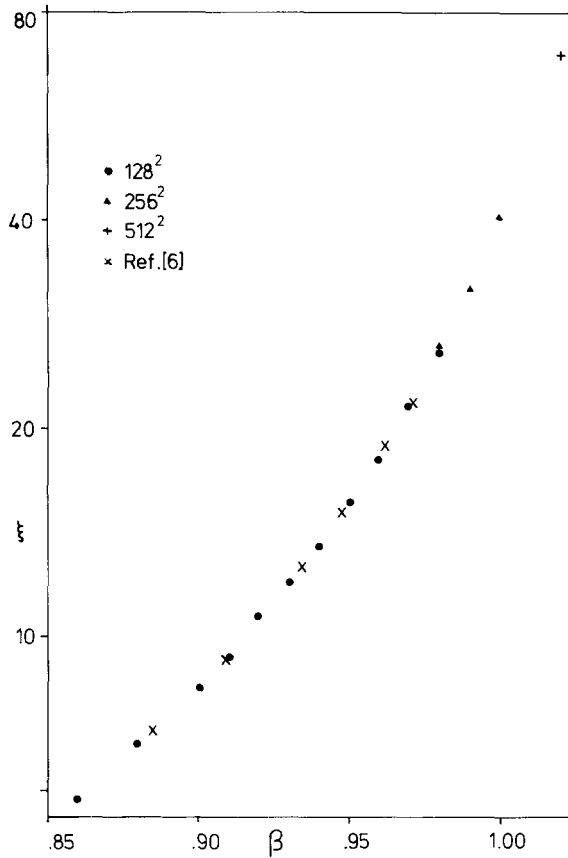


Fig. 1. Correlation length ξ versus β in the vortex phase. Errors correspond roughly to the size of the symbols.

results of ref. [6] are shown for comparison, too. At $\beta = 0.98$ ($\xi \cong 26$) there are two data points corresponding to lattice sizes $L = 128$ and 256 . Although close to each other, the two values show a small finite-size dependence somewhat above the level of our errors. Since we are interested in the infinite-volume limit, we clearly use the larger lattice here and keep L/ξ safely larger than about 6 for the other points. All quoted correlation lengths are derived from the zero (spatial) momentum timeslice correlation function. It is fitted by a hyperbolic cosine (appropriate for the periodic lattice) over a selfconsistently chosen range from ξ to the maximal distance $\frac{1}{2}L$. In each case we convinced ourselves that a fit starting from 2ξ gives the same result within statistical errors. The latter are estimated by subdividing our runs with typically several 10^5 measurements of direct correlations into 2, 4, ..., 128 subsamples. For each of them the fits and other nontrivial combinations of primary observables are made, and their fluctuations are observed and give the errors. In

TABLE 1
Numerical results of simulations in the vortex phase

β	L	$\frac{t_{\text{run}}}{1000}$	τ_χ	τ_{nn}	χ	ξ	C_v
0.82	56	30.2			36.33(14)	4.315(27)	
0.86	128	15.2	0.139(2)	2.4(2)	59.85(26)	5.843(38)	1.265(22)
0.88	128	25.5	0.135(1)	2.4(2)	80.58(31)	7.011(40)	1.326(21)
0.90	128	21.3	0.139(2)	2.7(2)	111.43(44)	8.476(66)	1.344(22)
0.91	128	25.6	0.140(2)	2.7(2)	134.17(45)	9.360(53)	1.392(20)
0.92	128	24.7	0.147(2)	2.9(2)	162.68(61)	10.69(8)	1.432(20)
0.93	128	50.9	0.152(3)	2.8(2)	201.29(53)	12.03(6)	1.413(15)
0.94	128	31.7	0.165(2)	3.0(3)	249.9(0.8)	13.50(9)	1.445(19)
0.95	128	40.7	0.182(2)	3.0(2)	319.6(1.1)	15.61(10)	1.436(19)
0.96	128	26.1	0.211(3)	3.3(2)	414.1(1.7)	18.08(13)	1.447(22)
0.97	128	28.2	0.268(4)	3.6(2)	554.9(2.9)	21.66(13)	1.445(21)
0.98	128	37.9	0.358(5)	3.7(1)	744.1(3.0)	25.84(15)	1.464(20)
0.98	256	28.9	0.148(1)	3.8(2)	764.6(3.0)	26.37(19)	1.491(22)
0.99	256	27.6	0.172(2)	3.8(2)	1092(4)	31.78(21)	1.404(19)
1.00	256	60.9	0.223(2)	4.0(2)	1604(4)	40.19(18)	1.444(16)
1.02	512	14.0	0.171(3)	4.1(5)	4170(19)	69.27(59)	1.311(27)

Runtime t_{run} and integrated autocorrelation times τ_χ of the susceptibility and τ_{nn} of the nearest-neighbor correlation refer to the unit “flip per spin”. Also shown are the correlation length ξ and, for completeness, the specific heat C_v . Errors are 1σ in all tables.

table 1 all results for χ , ξ and the specific heat C_v are collected. We also quote values for the integrated autocorrelation times τ_χ for χ and τ_{nn} for the nearest neighbor correlation. For any quantity with a connected autocorrelation function between successive measurements $\Gamma(t)$, τ is defined as

$$\tau = \frac{1}{2\Gamma(0)} \sum_{t=-W}^{t=W} \Gamma(t). \tag{3.1}$$

Here W is a suitably defined window, to which the infinite summation has to be truncated as discussed in ref. [8]. It was selfconsistently taken to be larger than 6τ . Errors on τ were also computed following ref. [8], appendix C. The practical importance of τ derives from the fact that 2τ is the factor by which naive rms errors have to be scaled up due to autocorrelations. At each β our measurements are separated by a fixed number of update steps chosen such that an average of about fL^2 spins are flipped with f around 0.1. These measurements are correlated on a timescale $\bar{\tau}$ between 1 and about 3. In table 1 $\tau = f\bar{\tau}$ is quoted which thus refers to units comparable to the sweeps of a local Metropolis algorithm as far as CPU effort is concerned. Another check on integrated autocorrelations is provided by comparing errors of simple observables estimated by the binning procedure. To actually

determine τ in this way is, however, unnecessarily inaccurate as the window is effectively given by the subsample block size [8]. We first also planned a column in table 1 showing the average size $\langle |C| \rangle$ of clusters in the update steps. It turned out, however, that it is well represented within statistical errors by the formula $\langle |C| \rangle \cong 0.81\chi$ for all β in table 1 and also for values that will appear in the spinwave phase. The constancy of the coefficient – it is exactly equal to 1 in the Ising model [1] – demonstrates nicely that our clusters are directly coupled to the physics of the model. A similar behavior was observed in simulations of the O(3) model.

The observed values of τ_χ indicate that it is a universal function of ξ/L . This is apparent if one compares for instance data points at $\beta = 0.95$, $L = 128$, $\beta = 0.99$, $L = 256$, and $\beta = 1.02$, $L = 512$, which have very similar τ_χ values. In other words, critical slowing down is completely absent for physical simulations where one makes L and ξ grow in the same proportion. Moreover $\tau_\chi \cong 0.14$ for $\xi/L \cong 0$ is a pleasantly small value showing that even for small correlation lengths the new algorithm is very efficient. The autocorrelation time τ_{nn} of the correlation at the shortest nontrivial distance possible shows a gradual increase with ξ comparable to the SW algorithm. Its growth is intuitively understandable as the scalar product of nearest-neighbor spins are only changed if they become part of a cluster surface. As the typical clusters grow large this happens less often. In principle local sweeps could be tried to speed up the short-wavelength modes, but we found no necessity to do so.

We further analyze our data by investigating the relation between χ and ξ as β approaches β_c from below. To check if eq. (1.4) is obeyed we plot in fig. 2 $\log(\chi/\xi^{7/4})$ versus $\log(\xi)$. Had η the KT value $\frac{1}{4}$, then we should find a horizontal

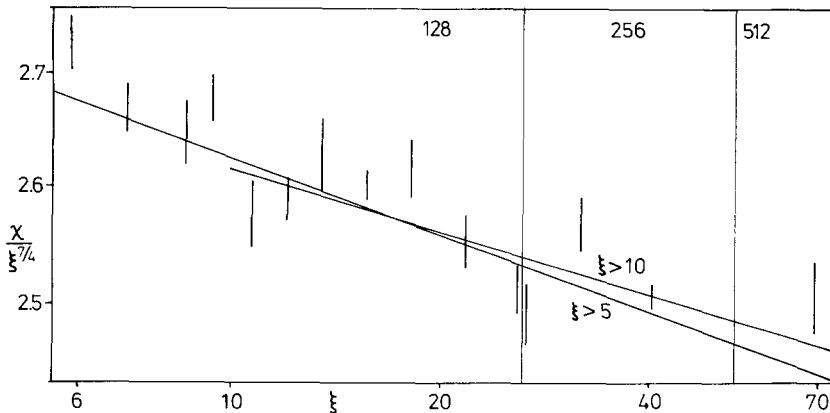


Fig. 2. Connection between magnetic susceptibility χ and correlation length ξ . Errors in this plot (only) are 2σ . They have been neglected for ξ and determined by the binning procedure directly for the combination $\chi/\xi^{7/4}$. The numbers on the top give the lattice size. Two different least-square fits deleting smaller ξ are shown.

line. A straight line of nonzero slope $-\Delta\eta$ corresponds to eq. (1.4) with $\eta = \frac{1}{4} + \Delta\eta$. One sees a clear tendency for a negative slope in fig. 2. We performed two different straight-line fits using only points with $\xi > 5$ and $\xi > 10$:

$$a = 1.05(1), \quad \eta = 0.287(3), \quad \chi^2_{LS} = 26.7 \quad (13 \text{ dgf}), \quad \xi > 5$$

$$a = 1.03(1), \quad \eta = 0.280(4), \quad \chi^2_{LS} = 20.0 \quad (9 \text{ dgf}), \quad \xi > 10$$

$$\text{in } \log(\chi/\xi^{7/4}) = a - \Delta\eta \log(\xi), \quad (3.2)$$

where χ^2_{LS} is the sum of the squared residues. Even with improved simulation possibilities it remains of course undecided in a numerical calculation whether closer to the transition point at – say – $\xi = 10^5$ the KT value for η will be assumed. In ref. [9] it has in fact been argued that for KT like systems such an extreme proximity to the transition point may be required. Note that eq. (3.2) shows the tendency toward a lower η as more data at smaller ξ are ignored.

We finally fit χ versus β to the form (1.3). In the actual fit we use (1.3) for the logarithm

$$\log(\chi) = c_x + b_x(1 - \beta/\beta_c)^{-\nu}. \quad (3.3)$$

This has the advantage that in the least-square minimization c_x and b_x occur as linear parameters. They are easily optimized for any fixed values of β_c and ν , and we only have to use nonlinear optimization in two or, if ν is frozen, in one parameter. Although trivial we found that this strategy is far superior to the use of general nonlinear fit routines for three and four parameters. In fig. 3 we see the least-square χ^2_{LS} as a function of ν with the three other parameters of eq. (3.3) always at their optimal values. Again we fit in the modes with only $\xi > 5$ and with $\xi > 10$. The crosses result from analogous fits with the asymptotic KT form written in the temperature rather than β , i.e. fitting

$$\log(\chi) = c'_x + b'_x(\beta'_c/\beta - 1)^{-\nu}. \quad (3.4)$$

We find reasonable minimal χ^2_{LS} values for all fits and for $\xi > 10$ also consistency between the two asymptotically equivalent parametrizations. This is only marginally the case for $\xi > 5$, which thus indicates the presence of deviations from KT scaling due to finite lattice spacing effects. But even in this case the difference between eqs. (3.3) and (3.4) is much less than what is reported in ref. [6]. A plausible estimate for ν on the basis of fig. 3 is $\nu = 0.45(+0.25/-0.15)$ with errors given by $\Delta\chi^2_{LS} = 1$. Table 2 displays results from a number of fits for eq. (3.3) with both frozen ν and with four free parameters. Errors on these fit parameters are derived by modelling the fluctuations of the input data by a normal distribution with the observed variance and repeating the fit many times. An important observation from table 2 is

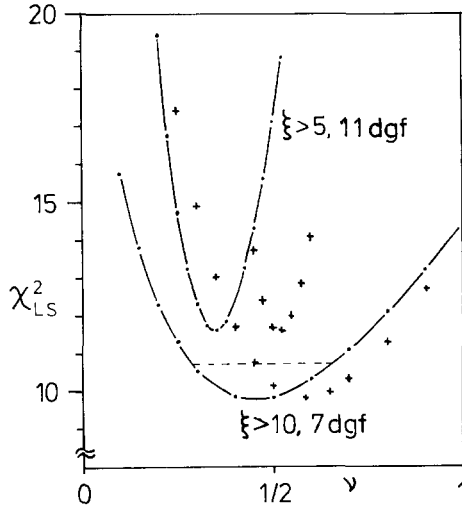


Fig. 3. The sum of least squares in fitting $\chi(\beta)$ to the KT form (3.3) for various values of ν (dots connected by lines to guide the eye). Two different subsets of data from table 2 are used as indicated. The crosses were obtained by fitting with (3.4) and map out similar curves shifted to slightly higher ν .

that, when ν is fitted, c_x and b_x remain almost undetermined, and also β_c is much less well determined. This proves almost-flatness of the χ^2_{LS} landscape in some directions corresponding to joint deformations of our fit parameters. Would one vary them one at a time, clearly a much smaller but totally unrealistic error-estimate would result. Table 2 entries with $\nu = 0$ correspond to a conventional critical point

$$\log(\chi) = \text{const.} - \tilde{\nu} \log(\beta_c - \beta). \tag{3.5}$$

TABLE 2
Results from fits of $\chi(\beta)$ to the KT form (3.3)

ξ_{\min}	χ^2_{LS}	ν	β_c	b_x	c_x
> 5	11.6	0.35(8)	1.11(4)	6(2)	-6(2)
> 5	17.1	0.5	1.128(5)	3.57(4)	-3.24(5)
> 5	76.0	0	1.074(8)		$\tilde{\nu} = 3.1$
> 10	9.76	0.45(25)	1.12(7)	4(10)	-4(10)
> 10	9.83	0.5	1.13(1)	3.5(1)	-3.1(2)
> 10	10.8	0.28	1.10(1)	8.0(3)	-8.2(3)
> 10	10.8	0.67	1.14(2)	2.2(1)	-1.5(2)
> 10	21.7	0	1.08(1)		$\tilde{\nu} = 3.2$

Where ν is quoted with errors four parameters (incl. ν) were fitted, otherwise ν was frozen to the value given.

As in ref. [2] we find that it leads to a lower estimate for β_c . Since χ_{LS}^2 is higher by at least 12 units we think that this fit is excluded. Also the rather large values for $\tilde{\nu}$ seem to show that the data demand a strong singularity.

4. Numerical results in the spinwave phase

We now come to x - y model results above and deeply in the transition region where the finite size of the periodic lattice is the smallest or the only mass scale. Data from these runs are compiled in table 3. With sizes $L = 32, 64, 128$ for each β we can check relation (1.6) by plotting $\log(\chi)$ against $\log(L)$ as done in fig. 4. We find good linearity and determine η by fits (see table 4). The slight deviation from linearity at $\beta = 1.07$ is taken into account by a larger error. Note, that $\beta = 1.07$ is still expected to produce the vortex phase in infinite volume. Autocorrelation times are listed in table 3 in the same units as in sect. 3. We see a slow increase of τ_χ with β but no strong L -dependence at fixed β . As mentioned before, the average size of the clusters is given by $\langle |C| \rangle \cong 0.81\chi$ in all runs including the asymmetric ones ($T \neq L$, see below).

TABLE 3a
Data for larger β -values Q^2 is the thermal average of the global U(1) charge squared

β	L	$\frac{t_{\text{run}}}{1000}$	τ_χ	τ_{nn}	χ/L^2	Q^2	C_v
1.07	32	83.1	1.56(3)	3.4(2)	0.3958(4)	0.6070(12)	1.072(9)
1.07	64	33.7	1.32(5)	3.6(3)	0.3245(5)	0.5776(17)	1.067(14)
1.07	128	20.3	1.12(4)	3.8(5)	0.2608(5)	0.5433(24)	1.105(20)
1.12	32	222.0	1.60(2)	3.5(1)	0.4420(2)	0.7096(5)	
1.12	64	79.6	1.40(3)	3.6(1)	0.3754(3)	0.6997(9)	
1.12	128	51.6	1.26(3)	3.8(2)	0.3190(3)	0.6900(9)	
1.30	32	112.0	2.12(4)	5.2(2)	0.5383(3)	0.9622(4)	0.757(5)
1.30	64	49.8	1.86(5)	4.6(2)	0.4794(4)	0.9613(4)	0.757(9)
1.30	128	22.1	1.95(9)	5.1(3)	0.4275(5)	0.9602(6)	0.779(14)
1.50	32	126.0	2.47(5)	6.1(2)	0.6053(3)	1.1892(3)	0.660(6)
1.50	64	57.3	2.50(8)	6.6(3)	0.5517(4)	1.1883(3)	0.665(9)
1.50	128	25.9	2.44(12)	6.9(8)	0.5017(5)	1.1885(4)	0.670(13)

TABLE 3b
Some results on asymmetric $L \times T$ lattices

β	L	T	τ_χ	χ/LT	Q^2	ξ
1.12	32	256	0.52(2)	0.1706(10)	0.08782(14)	44.1(5)
1.50	32	256	1.3(2)	0.3526(15)	0.14860(4)	76.5(8)

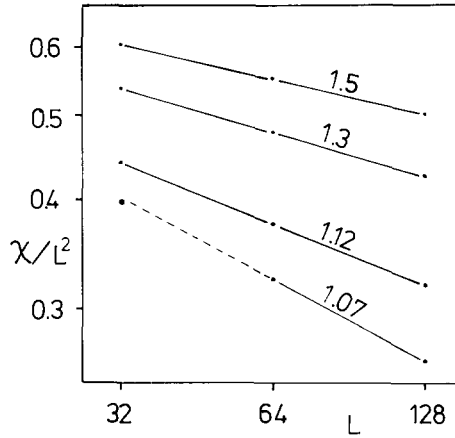


Fig. 4. $\log(\chi/L^2)$ versus $\log(L)$ for several β -values.

At large β we expect the x - y model to be solvable by perturbation theory. In contrast to the nonabelian $n > 2$ σ -models there are no perturbative ultraviolet divergences in this case. This leads to a vanishing β -function, and the continuum limit should be reached at fixed finite β . Of course, still only suitable long-range quantities (as compared to the lattice spacing) will become universal. This in particular necessitates taking $L \rightarrow \infty$ to truly get rid of lattice artifacts. In this limit a one parameter family of continuum models arises that may for instance be labelled by η . We use $(2\pi\eta)^{-1} = \beta_R$ as a renormalized inverse coupling. For $\beta \rightarrow \infty$ we know from spinwave analysis [4] that $\beta_R = \beta[1 + O(1/\beta)]$ holds. We may also use Wilson type renormalization group arguments in a direct way. A Villain action written for the spin angles φ_x ,

$$Z = \prod_x \int_0^{2\pi} d\varphi_x \exp\left(-\frac{1}{2}\beta_V \sum_{x\mu} (\varphi_{x+\mu} - \varphi_x |_{\text{mod } 2\pi})^2\right), \quad (4.1)$$

TABLE 4

Values for η from fits to data points shown in fig. 4 and corresponding values $\beta_R = (2\pi\eta)^{-1}$.
The last columns are zero and one-loop mean field calculations for β_R

β	η	β_R	β_R^{MF0}	β_R^{MF1}
1.07	0.304(4)	0.524	0.769	0.723
1.12	0.2325(7)	0.685	0.823	0.782
1.30	0.1665(9)	0.956	1.013	0.983
1.50	0.1350(7)	1.179	1.221	1.197

is expected to lie in the same universality class as eq. (1.1) for $n = 2$ since it keeps all symmetries and drops only irrelevant terms. Then there should be a choice of the only coupling $\beta_V(\beta)$ producing the same long-range physics. For this action the lowest-order spinwave calculation is exact up to terms exponentially small in β_V from the compactness of the angles. We conjecture that β_R and β_V agree to all orders in $1/\beta$. We may then evaluate all physical quantities with the Villain action and the renormalized coupling. This is nothing but a way to set up a renormalized perturbation expansion for continuum physics.

To assess the validity of the above picture, we looked at two types of physical quantities apart from η . The first is the finite volume mass gap induced by the toroidal spatial geometry, that – as emphasized by Lüscher [10] – can be used as a convenient probe of universal physics. We now consider an asymmetric $L \times T$ lattice with $T \gg L$. Eq. (4.1) gives us an effective action for the spatially constant modes φ_t , $t = 0, \dots, T - 1$,

$$-S_{\text{eff}}[\varphi_t] = \frac{1}{2}\beta_V L \sum_t (\varphi_{t+1} - \varphi_t|_{\text{mod } 2\pi})^2. \tag{4.2}$$

With $-\pi \leq \varphi_t \leq \pi$ the integral over these modes is recognized as the euclidean Feynman path integral for a particle on a circle with hamiltonian

$$H_{\text{eff}} = -(2\beta_V L)^{-1} \partial^2 / \partial \varphi^2. \tag{4.3}$$

Its gap $(2\beta_V L)^{-1}$ equals the inverse correlation length as it is defined in this paper. This coincides with the general small-volume results [10] for $n = 2$. Note that in the abelian model any finite volume is physically small in some sense. Since no coupling between zero momentum and other modes occurs, eq. (4.3) may be used for all L . Comparison between $\beta_V \cong \beta_R$ from table 4 and mass gap results ξ at $L = 32$ in table 3 gives evidence for agreement within errors.

A second type of physical observable makes use of the global $U(1) = SO(2)$ symmetry of the model. We may diagonalize the associated charge Q simultaneously with the transfer matrix $\exp(-H)$. It was shown in ref. [11] how thermal averages of powers of Q are related to simple euclidean correlation functions. The generating function is

$$\langle\langle e^{i\gamma Q} \rangle\rangle = \frac{\text{Tre}^{-TH+i\gamma Q}}{\text{Tre}^{-TH}} = \frac{Z_\gamma}{Z_0}, \tag{4.4}$$

where Z_γ is the partition function with twisted boundary conditions in euclidean time

$$\sigma_{x+T\hat{2}} = e^{\gamma l} \sigma_x \tag{4.5}$$

using the real matrix generator $I = \begin{pmatrix} 0 & 1 \\ -1 & 0 \end{pmatrix}$ of the $SO(2)$. Comparing coefficients of γ^2 we find the charge square related to a combination of the temporal nearest-neighbor correlation and a current susceptibility

$$\langle\langle Q^2 \rangle\rangle = (\beta/T^2) \left[\sum_x \langle \sigma_x \cdot \sigma_{x+\hat{z}} \rangle - \beta \left\langle \left(\sum_x \sigma_x \cdot I \sigma_{x+\hat{z}} \right)^2 \right\rangle \right]. \tag{4.6}$$

We measured Q^2 in all runs. Whenever $\xi \ll L, T$ one finds $Q^2 = 0$ within errors which simply shows that the vacuum is neutral. In the spinwave phase Q^2 becomes measurable and independent of $L = T$ at larger β (see table 3). It assumes its continuum limit as $T, L \rightarrow \infty$ which can only depend on β and T/L for dimensional reasons. Our data thus corroborate the existence of the continuum limit at fixed β in the spinwave phase.

For a theoretical calculation of Q^2 we employ again the Villain action (4.1). A simple perturbative calculation gives

$$Z_\gamma = \exp\left(-\frac{1}{2}\beta_V \frac{L}{T} \gamma^2\right), \quad Q^2 = \beta_V \frac{L}{T}. \tag{4.7), (4.8)}$$

Again data in tables 3 and 4 ($\beta_V \cong \beta_R$) agree reasonably well with this formula.

Finally, we discuss a possibility to get some control over the finite relation between bare coupling β and the renormalized β_R . It turns out that perturbation theory in $1/\beta$ exhibits bad convergence which is not surprising in the range of relevant β . We found the expansion around the mean field [12] more successful. When re-expanded in $1/\beta$ the perturbative information is contained in it too. The same experience has been discussed in ref. [11]. To set up this expansion we compute Z_γ as the saddle point (SP) approximation of

$$Z_\gamma = \prod_x \int_{-\infty}^{\infty} d^2\sigma_x \int_{-i\infty}^{i\infty} (2\pi i)^{-2} d^2\alpha_x \\ \times \exp\left\{ \sum_x \left[\beta(\sigma_x \cdot \sigma_{x+\hat{1}} + \sigma_x \cdot e^{I\gamma/T} \sigma_{x+\hat{z}}) + W(|\alpha_x|) - \sigma_x \cdot \alpha_x \right] \right\} \tag{4.9}$$

with the Fourier transform of the original measure on the circle given by a modified Bessel function

$$W(|\alpha|) = \log[I_0(|\alpha|)]. \tag{4.10}$$

Variables have been changed in eq. (4.9) such that all fields are periodic now. We shift the α -contours to pass through the constant real saddle point $(\sigma_0 m, \alpha_0 m)$

where m is some direction on S_1 , and (σ_0, α_0) obey the SP equations

$$\sigma_0 = W'(\alpha_0), \quad \alpha_0 = 2\beta(1 + \cos(\gamma/T))\sigma_0. \quad (4.11)$$

The SP approximation yields then to order γ^2

$$Z_\gamma \propto \exp\left(-\frac{1}{2}\beta\sigma_0^2\gamma^2L/T\right), \quad Q^2 = \beta\sigma_0^2L/T, \quad (4.12), (4.13)$$

where σ_0 is now given by solving (4.11) with $\gamma = 0$. Using eq. (4.8) we see β_R to be approximately given by

$$\beta_R^{\text{MF0}} = \beta\sigma_0^2, \quad (4.14)$$

which is also evaluated in table 4 and represents a much better approximation than the leading perturbative result $\beta_R \cong \beta$. We also analysed the gaussian fluctuations around the SP in eq. (4.9). The calculation is a little lengthy but straightforward. The resulting determinant has an infrared finite γ -dependence whose infinite lattice limit leads to the corrected β_R^{MF1} . When re-expanded in $1/\beta$ one finds that the first perturbative correction is fully contained in β_R^{MF0} , and the one-loop term starts only in the next order. We strongly recommend also for other models to use the mean field as a resummation technique for lattice perturbation theory if one wants to look for asymptotic scaling in the bare parameters.

5. Conclusions

The most important result of the present study of the $x-y$ model is the confirmation that the new collective Monte Carlo technique completely eliminates the problem of critical slowing down. This is particularly welcome for two-dimensional models where already on presently existing computers slowing down had become the main obstacle to progress in physically interesting simulations. It is remarkable that the complexity of operations needed for updating is entirely comparable to that of standard local algorithms. We hope to develop similar schemes for gauge theories, where the problem will become similar with future supercomputers.

The physics of the $x-y$ model could be studied in new regimes closer to the transition region. The Kosterlitz–Thouless behavior is confirmed and a conventional critical point excluded. We approach the critical temperature to within 10% corresponding to correlation lengths up to 69 in the vortex phase. In this range the critical exponent η , defined from the scaling relation between susceptibility and correlation length, exceeds the KT value $\frac{1}{4}$. There are theoretical arguments [9] that suggest that this may still be due to deviations from scaling, i.e. to a too small correlation length. With the new algorithm one could clearly simulate still bigger systems with the main limitation being computer memory. Such a calculation would be considerably further simplified by the use of reduced variance estimators that we

discovered in the meantime in conjunction with the cluster update scheme. This will be reported on in the near future together with results in the $O(3)$ model [13]. In the spinwave phase the x - y model was found to behave as expected on perturbative grounds.

An exchange with Alan Sokal and Erhard Seiler improved this work considerably. Also helpful were conversations with A. Burkitt, D. Heerman, I. Montvay, F. Niedermayer, and F. Wagner. Finally the author would like to thank the DESY theory group for their hospitality. The simulations were carried out on the Cray X-MP/18 and VAX 8550 at Kiel University.

References

- [1] U. Wolff, *Phys. Rev. Lett.* 62 (1989) 361
- [2] A. Patrascioiu, E. Seiler and I.O. Stamatescu, MPI München preprint MPI-PAE/PTh 75/87;
A. Patrascioiu, E. Seiler, I.O. Stamatescu, and V. Linke, *Nucl. Phys.* B305 [FS23] (1988) 623
- [3] J.M. Kosterlitz and D.J. Thouless, *J. Phys.* C6 (1973) 1181;
J.M. Kosterlitz, *J. Phys.* C7 (1974) 1046
- [4] J.B. Kogut, *Rev. Mod. Phys.* 51 (1979) 659
- [5] J. Tobochnik and G.V. Chester, *Phys. Rev.* B20 (1979) 3761;
J.E. Van Himbergen and S. Chakravarty, *Phys. Rev.* B23 (1981) 359;
J.F. Fernandez, M.F. Ferreira and J. Stankiewicz, *Phys. Rev.* B34 (1986) 292
- [6] R. Gupta, J. DeLapp, G. Batrouni, G.C. Fox, C.F. Baillie and J. Apostolakis, *Phys. Rev. Lett.* 61 (1988) 1996
- [7] R.H. Swendsen and J.S. Wang, *Phys. Rev. Lett.* 58 (1987) 86
- [8] N. Madras and A.D. Sokal, *J. Stat. Phys.* 50 (1988) 109
- [9] J.M. Greif, D.L. Goodstein and A.F. Silva-Moreira, *Phys. Rev.* B25 (1982) 6838;
J.L. Cardy, *Phys. Rev.* B26 (1982) 6311
- [10] M. Lüscher, *Phys. Lett.* B118 (1982) 391
- [11] U. Wolff, *Nucl. Phys.* B265 [FS15] (1986) 537
- [12] J.M. Drouffe and J.B. Zuber, *Phys. Rep.* 102 (1983)
- [13] U. Wolff, DESY-Report 89-021 (February 1989)